Two Peptides Derived from the Nerve Growth Factor Precursor Are Biologically Active

Eleni Dicou,* Beth Pflug,‡ Marilyn Magazin,§ Thérèse Lehy,‖ Daniel Djakiew,‡ Pascual Ferrara,§ Véronique Nerrière,* and Douglas Harvie*

*Institut National de la Santé et de la Recherche Médicale U298, Centre Hospitalier Universitaire, Angers 49033, France; ‡Department of Cell Biology, Georgetown University Medical Center, Washington DC, 20007;§Sanofi Recherche, 31676 Labège, France; and ‖Institut National de la Santé et de la Recherche Médicale U10, Hôpital Bichat, 75877 Paris, Cedex 18, France

Abstract. This report provides evidence that the proregion of the NGF precursor protein contains two novel bioactive peptides. The presence of pairs of basic amino acid (aa) residues in the NGF proregion suggests that two or three peptides other than NGF may be generated by proteolytic cleavage. Synthetic peptides of 29 aa (LIP1) and 38aa (LIP2) corresponding to the sequences −71 to −43 and −40 to −3 of the proNGF, respectively, were used in this study. ELISA specific for these two peptides revealed their presence in the rat intestine. LIP1 was localized by immunohistochemistry in endocrine cells of the intestinal epithelium, and LIP2 was immunoprecipitated from an intestinal extract. We also provide evidence for the presence of specific receptors for LIP2 in several cell lines. Scatchard analysis indicated the presence of a low affinity binding site with a K_d of $\sim 10^{-7}$ M and a high affinity binding site of 10^{-9} M. Cross-linking studies revealed receptor forms of about 140 kD and 93 kD in a prostatic adenocarcinoma cell line.

LIP1 and LIP2 induced rapid F-actin redistribution in PC12 cells within 2 min of incubation, which suggests a role of LIP1 and LIP2 in the process of neurite outgrowth. Furthermore, both propeptides induced rapid tyrosine phosphorylation of the Trk protein in both prostatic adenocarcinoma cells and PC12 cells, thus implicating *trk* in their mechanism of action. These results support our hypothesis that two peptides within the NGF precursor protein are biologically active.

NGF and the NGF family of neurotrophins regulate the survival and differentiation of neurons in the peripheral and central nervous systems (Thoenen, 1991; Meakin and Shooter, 1992). The nucleotide sequence of the NGF cDNA, isolated from the mouse submaxillary gland (MSG)[1] contains two potential methionine initiation codons that can give rise to two precursor molecules: a long form of ~34 kD and a short form of 27 kD (Scott et al., 1983; Ullrich et al., 1983). Precursor forms of ~31 and 24 kD have been observed in vivo (Dicou et al., 1986; Dicou, 1992). The NGF moiety is situated at the COOH terminus and is flanked by dibasic amino acid (aa) processing sites. Formation of the mature 118aa NGF peptide requires proteolytic processing at both ends. Two other dibasic amino acids, representing potential processing sites, exist within the proregion that may generate two peptides, 29aa (LIP1) and 38aa (LIP2), from the short precursor and an additional 89aa peptide from the long precursor (Fig. 1). Liberation of the NH_2-terminal pre-propeptide from the long precursor was detected in vitro after digestion of the translation products of NGF mRNAs with γ-NGF, a trypsin-like subunit involved in the maturation of the MSG NGF (Dicou, 1989). In addition, in vitro mutagenesis studies suggested that two domains, situated within the proregion −53 to −26 and −8 to −2, may be important for the expression of active NGF (Suter et al., 1991).

It remained an open question whether the putative proNGF peptides have any biological role or whether they exist in vivo. To investigate these aspects, the two propeptides, LIP1 and LIP2, were chemically synthesized, and respective antibodies were raised in rabbits. The antibodies were used to develop specific ELISA. The synthetic peptides were used to characterize potential biological roles as well as to search for the presence of specific receptors.

Materials and Methods

LIP Peptides

Various peptides were purchased from Sigma Chemical Co. (St. Louis, MO). LIP1, a 29aa peptide, was synthesized by Neosystem SA (Strasbourg, France). LIP2, a 38aa synthetic peptide, was synthesized by Peninsula Labs. Europe, Ltd. (St. Helens, UK) Both peptides were purified to >95% purity, as estimated from the HPLC profile and verified by thin

Please address all correspondence to Eleni Dicou, INSERM U10, Hopital Bichat, 170 Boulevard Ney, 75877 Paris, Cedex 18, France. Tel.: 33-1-40-25-83-09. Fax.: 33-1-46-27-85-36.

1. *Abbreviations used in this paper*: aa, amino acid; ChAT, choline acetyltransferase; DRG, dorsal root ganglia; F-actin, filamentous actin; MSG, mouse submaxillary gland; NT, neurotrophin; PS, proteolytic site.

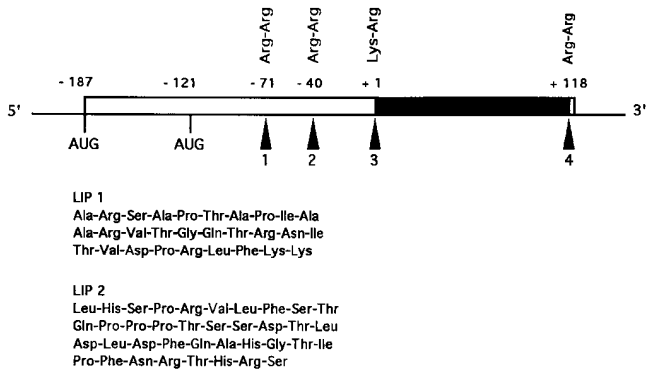

Figure 1. Schematic representation of the NGF precursor as deduced from the cDNA clone. The dark box is the NGF peptide. Arrows indicate possible proteolytic sites. AUG is the initiation methionine codon. LIP1 corresponds to the sequence between −71 to −43 and LIP2 corresponds to the sequence between −40 to −3 of the rat NGF precursor.

layer chromatography, amino acid analysis, HPLC (2 systems), and mass spectrometry. No significant homologies were found in the protein bank, NBRS (using the BLAST program), between these peptides and any known protein sequences other than to NGF precursor-related sequences.

Antibodies

Rabbits were immunized with peptides (1 mg) coupled to keyhole limpet hemocyanin (6 mg) with benzoquinone (Dicou et al., 1988). ELISA using immunoplates coated with 2 μg/ml of peptide in 0.1 M carbonate buffer, pH 9.2, was employed to test for the presence of specific antibodies in the sera, as described elsewhere (Dicou et al., 1989). The titer of the antipeptide antibodies was estimated to be ⩾1:200,000.

ELISA

Rabbit IgGs were purified by passage of polyclonal antibodies against LIP1 or LIP2 over a protein A column. ELISA plates (Nunc, Rostkilde, Denmark) were coated with 15 μg/ml purified rabbit IgG in 0.1 M carbonate buffer, pH 9.2, for 4 h at 37°C. Plates were washed five times with PBS-0.01% Tween. 100 μl of sample of either diluted synthetic peptide or tissue extract was pipetted into each well and incubated overnight at 4°C. Plates were then washed five times with PBS-0.01% Tween. Tissue extracts were tested at several serial dilutions. Part of the purified rabbit IgG was biotinylated with NHS-LC–Biotin (sulfosuccinimidyl-6-(biotinamido) hexanoate; Pierce, Rockford, IL) according to the manufacturer's instructions and used as a secondary antibody, at a concentration of 5 μg/ml in PBS-0.01% Tween–0.5% gelatin (PTG), for 2 h at 37°C. In specificity controls, unbiotinylated IgGs were added together with biotinylated IgGs at a ratio of 5:1, respectively. Plates were washed five times and incubated for 2 h at 37°C with avidin–peroxidase (Dako Corp., Carpinteria, CA) at 1:5,000 dilution in PTG. The reaction was visualized by adding 2,2′-Azino bis(3-ethylbenz-thiazoline-6-sulfonic acid) (ABTS; 1 mg/ml) as peroxidase substrate. The optical density was determined in a multiscan analyzer at an absorbance of 405nm. LIP1 and LIP2 values were calculated from absorbance data within the linear range of the calibration curve (Fig. 2) after subtracting the nonspecific background readings. This was done by including an excess of unbiotinylated antibody as the second antibody. Values are expressed in pg/mg protein of the tissue extract after centrifugation.

Chimeric β-galactosidase pre-proNGF was produced in *Escherichia coli*, harboring a bacterial vector with the fused preproNGF cDNA, and purified from the soluble fraction after cell lysis, as previously described (Dicou et al., 1989).

NGF was quantified with a two-site enzyme immunoassay using the monoclonal anti–mouse-β (2.5S) NGF antibody 27/21 (Boehringer Mannheim Biochemicals, Mannheim, Germany), as described previously (MacGrogan et al., 1992). From the standard curve, using purified mouse NGF, concentrations as low as 0.2 pg/well can be measured reproducibly.

Cell Extracts and Radiolabeling

Tissues were dissected from male Wistar rats (250 g) and homogenized with a Polytron homogenizer in 0.1 M borate buffer, pH 8.5, containing 1 mM phenylmethylsulfonylfluoride and 1 mM tosyl-L-lysine chloromethyl ketone (3 ml/g wet tissue). Homogenates were centrifuged at 100,000 *g* for 30 min, and the clarified supernatants were assayed by the specific ELISA and for protein content using a protein assay (Bio-Rad Laboratories, Inc., Richmond, CA).

About 100 μg of a rat intestinal extract that contained high LIP2 levels was radiolabeled with 50 μCi of ^{35}S-labeling reagent (Amersham Intl., Buckinghamshire, England), according to the manufacturer's instructions, for 30 min on ice. Subsequently, an additional 200 μg of extract was added, and incubation was continued for 30 min on ice. The reaction was stopped with 100 μl of 0.2 M glycine. In parallel, 10 μg of synthetic peptide was labeled with 50 μCi of ^{35}S-labeling reagent for 1 h on ice, and the reaction was stopped as above.

Immunoprecipitations

Half of the radiolabeled intestinal extract and ~2 μg of the labeled peptide were incubated with 10 μl of either anti peptide or preimmune serum and 100 μl of protein-A Sepharose, as previously described (Dicou, 1989). Immunoprecipitated complexes were analyzed by 18% SDS-PAGE (Laemmli, 1970) and subsequently by autoradiography.

Immunohistochemistry

Tissue samples of small intestine from adult Wistar rats were fixed in Bouin's solution at room temperature or in 4% paraformaldehyde in phosphate-buffered saline (0.1 M, pH 7.4) at 4°C for 18–24 h. They were routinely processed for dehydration, followed by paraplast embedding, and cut in 4-μm thick sections. Before immunoreaction, endogenous peroxidase activity was removed by dipping sections into 0.3% H_2O_2 in methanol for 30 min. Nonspecific binding of IgG was blocked by incubation in 10% normal goat serum. Thereafter, sections were incubated for 16 h at 4°C with anti-LIP1 serum, diluted 1:16, or with anti-LIP2, diluted 1:150–200. Sections were then incubated with goat biotinylated anti–rabbit IgG, diluted 1:200 for 30 min, and finally with the avidin–biotin complex, diluted 1:100 for 1 h (ABC Vectastain kit; Vector Labs Inc., Burlingame, CA). Negative controls were obtained by incubating tissue sections with preimmune serum. Specificity of the staining was checked by overnight preincubation of the anti-LIP1 or anti-LIP2 antiserum with 10, 20, or 40 μg of the homologous peptide/ml of diluted antisera.

Cell Lines

The human prostatic adenocarcinoma cell line, B5, derives from the tumorigenic DU-145 cell line after transfection with a normal retinoblastoma gene. This resulted in the loss of the capacity of B5 cells to form tumors (Bookstein et al., 1990). B5 cells were grown in DME with 10% FCS. PC12 cells (purchased from the American Type Culture Collection [ATCC]) and PC12 6-24 (Hempstead et al., 1992), overexpressing TrkA by 10–15-fold (gift of Dr. D. Kaplan, Montreal Neurological Institute, Montreal, Quebec, Canada), were grown in RPMI-1640 (GIBCO BRL Laboratories, Grand Island, NY) supplemented with 10% horse serum (HS) and 5% FCS. SH-SY5Y cells were grown in RPMI-1640 medium supplemented with 12% FCS, L-929 cells in DME supplemented with 5% FCS, Ros cells in F12 Ham's supplemented with 10% FCS, 6-23 cells in DME supplemented with 12% HS and 2.5% FCS, and Vero cells in RPMI-1640 supplemented with 10% FCS. For binding studies, cells were washed in PBS, scraped with a rubber policeman, collected by centrifugation, and resuspended in binding buffer.

Iodination

LIP2 (5 μg) was iodinated using 10 μg of chloramine-T (Sigma Chemical Co.) and 0.5–1 mCi of Na[^{125}I], sp act 15 mCi/μg (Amersham Intl.) in a total reaction volume of 50 μl in 0.25 M sodium phosphate buffer, pH 7.5, for 8 min at room temperature. The reaction was stopped with 500 μg of sodium metabisulphite, and unreacted iodide was removed by gel filtration on a PD10 column (Pharmacia Fine Chemicals, Piscataway, NJ) pre-equilibrated in PBS, 0.01% Tween-20. Specific activity was 300–500 cpm/fmol.

Binding Assay

Approximately 0.5–1 × 10^6 cells were incubated in binding buffer (PBS, 0.1% BSA), together with the appropriate concentrations of the iodinated peptide to give a final volume of 50 μl, in a 96-well, round-bottomed plate, with agitation, at 4°C or at room temperature. Samples were then layered

on a cushion of 150 μl of a 90% dibutyl phthalate and 10% mineral oil mixture (both Sigma Chemical Co.) in 400-μl microfuge tubes and centrifuged in a microfuge centrifuge (Beckman Instruments, Inc., Fullerton, CA) for 45 s. The tubes were frozen in liquid nitrogen and the tips (bound fraction) as well as the rest of the tube (free fraction) were removed and counted in a gamma counter. Nonspecific binding was determined in the presence of a 400–1,000-fold excess of peptide. Curve fittings were performed using the Graphit data analysis program (Erithacus Software Ltd., Staines, UK). In competition experiments, $\sim 10^6$ B5 and SH-SY5Y cells were preincubated with 2 μM of each competitor for 1 h at 4°C. [^{125}I]LIP2 was added at 10 nM and incubation continued. Specifically bound radioactivity was determined as above.

Cross-linking

About 10^7 cells were incubated in 200 μl binding buffer, containing 100 nM ^{125}I-LIP2, for 2 h at 4°C, either with or without 400-fold excess peptide. Cells were washed extensively in ice cold PBS, resuspended in 200 μl PBS, and incubated with 20 mM 1-Ethyl-3-(3-dimethylaminopropyl) carbodiimide (EDC; Pierce) for 30 min at room temperature. Cells were then washed twice in PBS and solubilized in Laemmli electrophoresis buffer. Proteins were resolved by 10% SDS-PAGE, followed by autoradiography on XAR-5 films (Laemmli, 1970).

Fluorescent Microscopy

PC12 and B5 cells were seeded into RPMI-1640 medium containing 1% HS in 15-ml slide flasks (coated with poly-D-lysine for PC12 cells). After 18 h of culture, cells were incubated for 2 min at 37°C in the presence of 10^{-7}, 10^{-8}, or 10^{-9} M peptide concentration or 100 ng/ml NGF. After washing with PBS, pH 7.4, cells were fixed with 3% paraformaldehyde (Merck Chemical Div., Rahway, NJ) for 20 min, washed, permeabilized in 0.1% Triton X-100 for 2 min, and then stained with a phallacidin–BODIPY or a phalloidin–rhodamine conjugate (Molecular Probes, Inc., Eugene, OR), using procedures similar to those described by Wulf et al. (1979). Slides were mounted with Vectashield medium (Vector Labs Inc.) and photographed with a microscope (Dialux 20; E. Leitz Inc., Rockleigh, NJ).

Neurite Outgrowth Bioassay

Dorsal root ganglia (DRG) were dissected from a 9-d-old chick embryo and cultured in the presence of 10^{-7}, 10^{-8}, and 10^{-9} M LIP1, LIP2, or with 10 ng of mouse NGF, as previously described (Dicou et al., 1993).

Trk Phosphorylation

The PC12 overexpressors of TrkA and B5 cells were grown to confluency in 150-mm plates. Cells were stimulated for 5 min with LIP1 or LIP2 (10^{-9} or 10^{-7} M in serum containing medium for LIP1 or 0.02% Tween for LIP2) or NGF (200 ng/ml, Genentech, Inc., South San Francisco, CA) and treated as previously described (Pflug et al., 1995). Cell lysates were immunoprecipitated with 4 μl of panTrk-21 antibody generated against the 14 COOH-terminal residues of the TrkA protein (Cephalon Inc., West Chester, PA). Immunoprecipitates were resolved by 7.5% SDS-PAGE and transferred onto a 0.2-μM nitrocellulose membrane. Blots were probed overnight at 4°C with an antiphosphotyrosine antibody conjugated to horseradish peroxidase (RC-20; Transduction Laboratories, Lexington, KY) at a 1:2,500 dilution in TBS supplemented with 0.1% Tween (TBST). Immunoreactivity was observed using enhanced chemiluminescence (ECL kit; Amersham Corp., Arlington Heights, IL). Blots were stripped (50 mM Tris, pH 6.5, 150 mM NaCl, and 2% β-mercaptoethanol) at 70°C for 1 h and reprobed overnight at 4°C with panTrk-203 antibody (Kaplan et al., 1991) at a 1:5,000 dilution in TBST. Goat anti–rabbit horseradish peroxidase–conjugated secondary antibody (Boehringer Mannheim Biochemicals) was used at a 1:20,000 dilution in TBST for 1 h at room temperature, followed by ECL.

Results

Detection of LIP1 and LIP2 by ELISA and Immunohistochemistry

The double-sandwich ELISA, specific for the two peptides, consisted of first coating microplates with purified polyclonal antibodies against LIP1 or LIP2. The sample containing appropriate dilutions of either the peptide solution or cell extract to assay was then added to form the primary antibody–antigen complex. As a secondary antibody, biotinylated polyclonal antibodies against LIP1 or LIP2 were used. The second antibody was revealed by the addition of avidin peroxidase, followed by the peroxidase substrate. The amount of LIP1 or LIP2 was calculated from a calibration curve that uses chemically synthesized LIP1 or LIP2 as a standard (Fig. 2). The detection limit for LIP1 is ~7 pg/well and for LIP2, ~4 pg/well. A specificity test was performed by the simultaneous addition of biotinylated and unbiotinylated antibodies as second antibody. This resulted in the extinction of the signal (Fig. 2).

The specificity of the ELISA was assessed against a panel of peptides and proteins. There was no cross-reaction against NGF, somatostatin, bradykinin, vasopressin, leucine enkephalin, methionine enkephalin, neurotensin, bombesin, angiotensin II, α-melanocyte stimulating hormone, and a peptide that reproduces the sequence −163 to −139 of the proNGF. In addition, there was no cross-reaction between LIP1 and LIP2 (data not shown).

In order to further verify that values measured by the ELISA assays correspond to the free peptides rather than proNGF sequences, the following control experiments

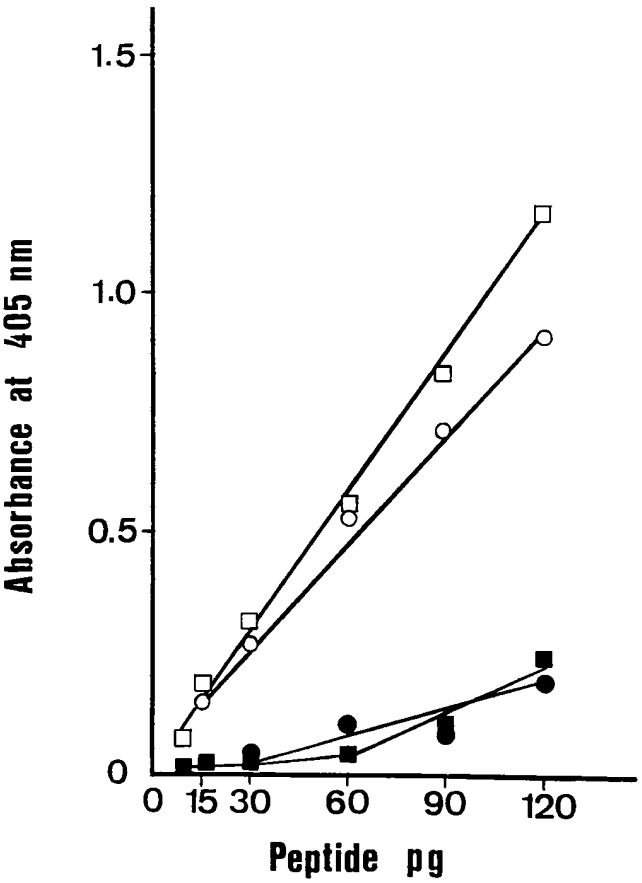

Figure 2. Calibration curve of the ELISA specific for the peptides. HPLC-purified synthetic peptides were used. The curve shows the linearity and sensitivity of the ELISA for LIP1 (□) and LIP2 (○). Peptide concentrations are in pg/well. The signal is strongly diminished in the presence of excess unbiotinylated antibodies (*dark symbols*).

Table I. Measurements of LIP1 and LIP2 by ELISA in Rat Tissues

	LIP1	LIP2
Heart	−	−
Spleen	−	−
Lung	−	−
Kidney	−	−
Liver	−	1.7 ± 1 (n = 4)
Intestine	8 ± 5* (n = 15)	67 ± 35* (n = 15)
Brain	−‡	−‡
Pancreas	−	−

Values are in pg/mg protein.
−Levels below the limit of detection. Negative tissues were obtained from two rats, and a total of four independent determinations were performed.
*Results were obtained from five rats.
‡Extract prepared from a brain hemisphere.

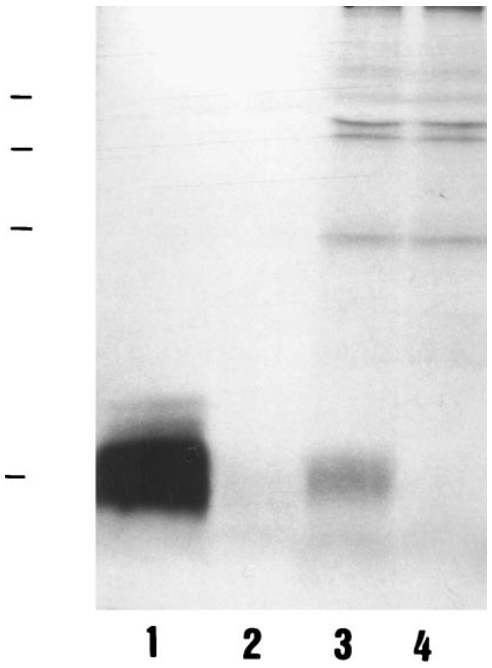

Figure 3. Immunoprecipitation of LIP2 peptide from a rat intestinal extract. Radiolabeled LIP2 synthetic peptide was immunoprecipitated with anti-LIP2 (lane *1*) or with preimmune serum (lane *2*). Radiolabeled rat intestinal extract was immunoprecipitated with anti-LIP2 serum (lane *3*) or with preimmune serum (lane *4*). Immunoprecipitates were fractionated by 18% SDS-PAGE, followed by autoradiography for 20 wk. Molecular weight markers are BSA (68 kD), ovalbumin (45 kD), α-chymotrypsinogen A (25 kD), and LIP2 (4.2 kD).

were performed. We have previously reported the synthesis of a chimeric β-galactosidase pre-proNGF protein in *Escherichia coli* (Dicou et al., 1989). LIP1 antibodies failed to cross-react with the chimeric pre-proNGF, while LIP2 antibodies cross-reacted with the pre-proNGF protein but to a lesser extent than with the peptide. The sensitivity of the ELISA was estimated to be about 25 times higher for LIP2 as compared to the precursor protein at equimolar concentrations of LIP2 and chimeric pre-proNGF. These in vitro results were also corroborated from measurements of LIP1 and LIP2 in extracts of the male MSG. The NGF mRNA content in this gland represents ~0.1% of the total mRNA, the highest in any other tissue. No LIP1 was detectable in these extracts, while LIP2 was estimated at about 2 ± 0.5 pg/mg protein (n = 4).

Using these ELISA tests, we examined several rat peripheral tissues for the presence of immunoreactive material (Table I). Most of the tissues examined was negative. Heart, spleen, and brain tissues, where expression of NGF mRNA is high, were negative. Some LIP2 was detectable in low amounts in the liver. The tissue that contained considerable levels of both peptides was the intestine. LIP2 like immunoreactive material was present in greater amounts as compared to LIP1. LIP1 and LIP2 seemed to be distributed along the small intestine, since extracts prepared separately from the duodenum, jejunum, and ileum all contained both peptides.

NGF was also measured in the intestinal extracts of two adult rats using a two site immunoassay, employing the monoclonal antibody 27/21 with a detection limit for NGF at about 0.2 pg/well. The estimated NGF was 0.15 ± 0.02 pg/mg protein (n = 4) for one rat and 0.18 ± 0.05 pg/mg protein (n = 4) for the second rat. The thermostability of the ELISA cross-reactive material was tested by heating intestinal extracts at 100°C for 1 h at pH 2. LIP1 and LIP2 activities were completely recovered, thus suggesting that they are temperature and acid resistant.

In order to determine whether food uptake physiologically influences mucosal content of LIP1 and LIP2, intestinal extracts from normally fed rats and from rats starved for 48 h were assayed for LIP1 and LIP2. There was a decrease of about 70 ± 5% (n = 4) of LIP1 and 96 ± 4% (n = 4) of LIP2 in extracts from food-deprived rats, as compared to their counterpart normally fed rats. In contrast, there was no change in NGF levels. NGF in the intestinal extract of a normally fed rat was estimated at ~0.10 ± 0.01 pg/mg protein (n = 4), as compared to 0.12 ± 0.01 pg/mg protein (n = 4) found in a starved rat.

Neither LIP1 nor LIP2 was detectable in an extract prepared from a brain hemisphere. However, some LIP2 was detectable in an extract prepared separately from the cortex (1.2 ± 0.1 pg/mg protein, n = 4), hippocampus (1.5 ± 0.3 pg/mg protein, n = 4), and septum (5 ± 1 pg/mg protein, n = 4), while an extract of the cerebellum was negative. LIP1 was undetectable in any of the brain regions examined.

Immunoprecipitations from an intestinal extract that contained 140 pg/mg protein of LIP2 and 19 pg/mg protein of LIP1 (not included in Table 1) yielded a band (Fig. 3, lane *3*) comigrating with the immunoprecipitated synthetic LIP2 peptide (lane *1*). This band was absent in immunoprecipitates with preimmune serum (lane *4*). We failed to detect immunoprecipitated LIP1, probably due to its lower levels.

Immunohistochemistry of tissue sections of the rat intestine localized LIP1 immunoreactivity in endocrine cells (Fig. 4). These cells were recognized by their ovoid or pyramidal shape, their position along the basement membrane, and the presence of a thin, cytoplasmic process extending to the gut lumen. They were relatively well represented, especially in the duodenal mucosa, and they were distributed both in villi and crypts, with a higher fre-

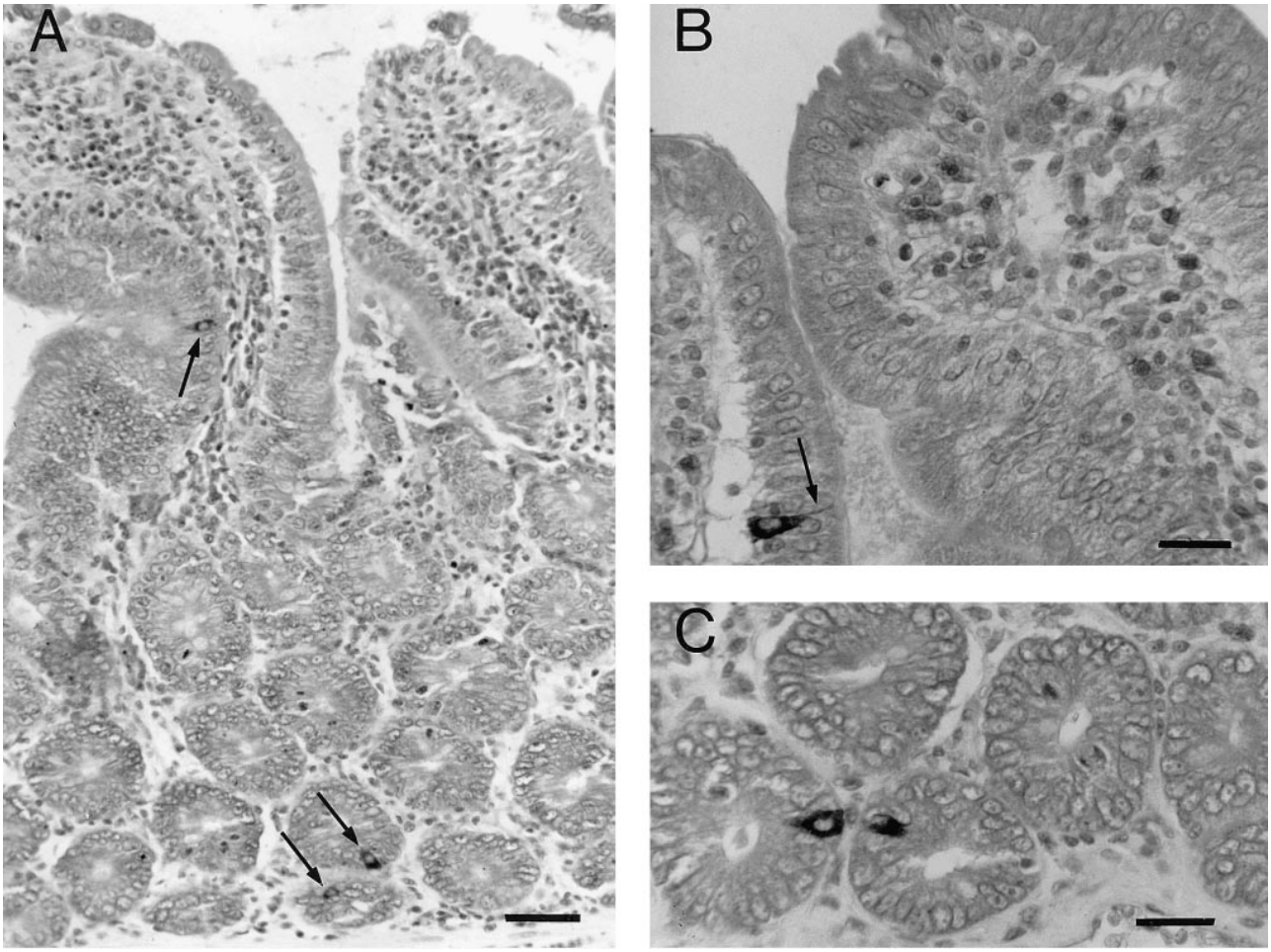

Figure 4. Localization of LIP1 immunoreactivity in the rat intestine. (*A*) General view of duodenal mucosa (Bouin-fixed tissue) showing LIP1-immunoreactive endocrine cells localized in crypt and villi (*arrows*). Nuclei were counterstained with Mayer's glychemalun. Bar, 20 μm. (*B* and *C*) Details of other LIP1-positive endocrine cells, one cell in a villus (*B*, *arrow*; this cell exhibits a characteristic cytoplasmic extension to the gut lumen) and two cells in crypts. Bar, 10 μm.

quency in the latter. Staining of LIP1-immunoreactive endocrine cells was decreased by prior absorption of antiserum with 10 μg/ml of homologous peptide and completely abolished by prior absorption with 20 μg/ml. Two polyclonal anti-NGF sera tested in parallel did not stain these endocrine cells, whereas they positively stained the convoluted tubules of the MSG, as previously described (Dicou et al., 1988). Weak to moderate anti-LIP2 immunoreactivity was found in epithelial cells of Brünner's glands and in villi and crypt cells. There was no staining of these cells with the corresponding preimmune serum, but preabsorption of the antiserum with the homologous peptide did not abolish the signal.

Binding of ^{125}I-LIP2 to Cell Lines

We screened several cell lines for the presence of receptors for LIP2 rather than LIP1, because LIP2 has three histidine residues, whereas LIP1 has no tyrosine or histidine residues for radioiodination. The prostatic adenocarcinoma cell line, B5, was previously shown to synthesize and secrete NGF (MacGrogan et al., 1992). Specific binding of ^{125}I-LIP2 was detected in B5 cells in a time and temperature dependent manner. At room temperature (~25°C) the peptide bound rapidly, reaching equilibrium in 30 min, whereas at 4°C it reached equilibrium in 2 to 3 h. Scatchard plot analysis showed the presence of a low affinity binding site, with a K_d of 48 ± 11 nM and 46,300 ± 6400 sites/cell (Fig. 5). Nonspecific binding represented less than 30% of total binding. In addition, a high affinity binding site with a K_d of 2.8 ± 0.1 nM and 7,057 ± 409 sites/cell was also detectable (Fig. 6). The low affinity binding constant obtained from analysis of Scatchard plots was also corroborated by displacement experiments in which cells were incubated simultaneously with a constant amount of ^{125}I-LIP2 (10 nM) and increasing amounts of nonradioactive LIP2, up to 2 μM for 2h at 4°C. The apparent K_d for the unlabeled peptide was about 2–4 × 10^{-7} M.

Other cell lines that bound ^{125}I-LIP2 included PC12 (rat pheochromocytoma) cells, 6-23 (rat medullary thyroid carcinoma) cells, SH-SY5Y (human neuroblastoma) cells, and HeLa (human cervical epithelioid carcinoma) cells. We failed to detect the high affinity component in SH-SY5Y and in HeLa cells. In the positive cell lines, the low affinity constant ranged between 10^{-7}–10^{-8} M and ~50,000–140,000 sites/cell, whereas the high affinity component

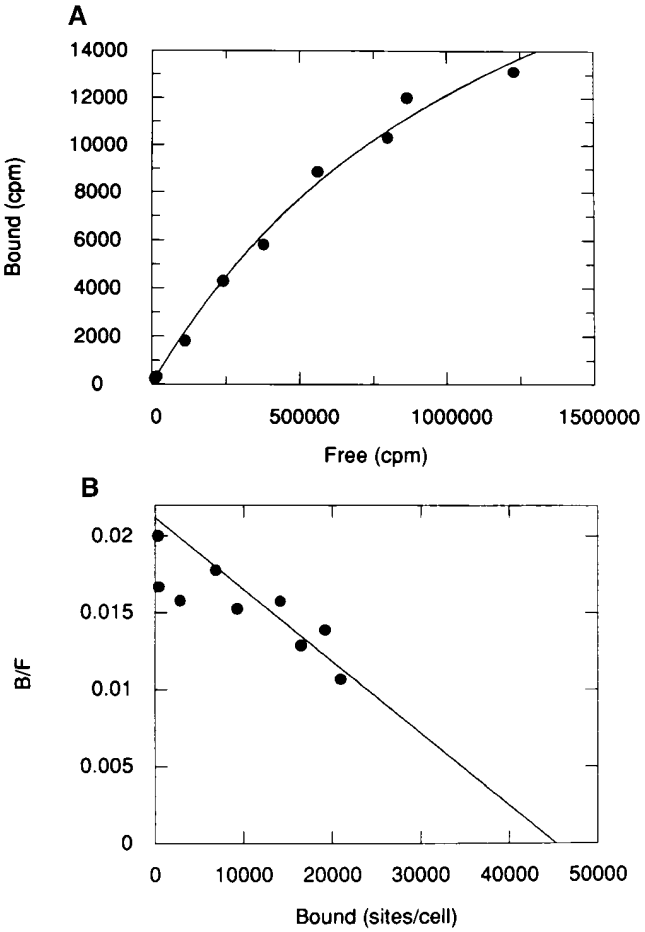

Figure 5. Low affinity binding of [^{125}I]LIP2 to B5 cells. (*A*) Increasing concentrations of ^{125}I-LIP2 were incubated for 2 h at 4°C with B5 cells (10^6 cells in 50 μl), and the bound and free fractions were determined as described in Materials and Methods. Specific binding is shown after subtraction of nonspecific binding from total binding. (*B*) Scatchard plot of the specific binding component. Curve fitting was as in Materials and Methods (estimated K_d = 48 ± 11 nM; B_{max} = 46,300 ± 6400 sites/cell).

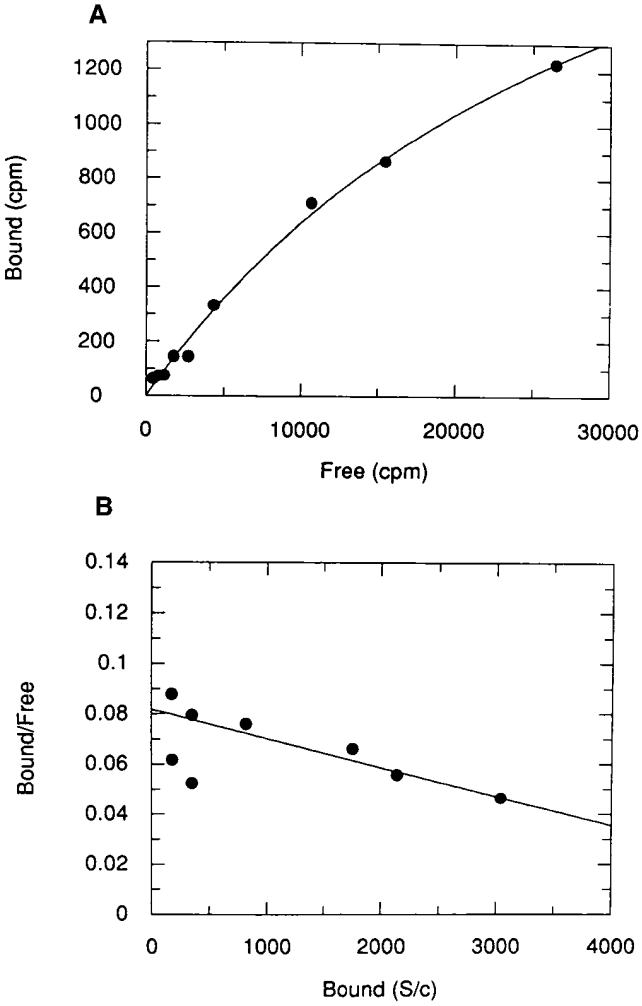

Figure 6. High affinity binding of ^{125}I-LIP2 to B5 cells. Experimental conditions are as in Fig. 4. (*A*) Specific binding. (*B*) Scatchard plot of the specific component (estimated K_d = 2.8 ± 0.1 nM; B_{max} = 7057 ± 409 sites/cell).

ranged between 0.5–2 × 10^{-9} M and 1000–7000 sites/cell. In contrast, several cell lines, including Vero (African green monkey kidney) cells, Ros (rat osteosarcoma), and L-929 (mouse fibroblast) cells, did not bind ^{125}I-LIP2.

The specificity of the LIP2 binding was further investigated by competition with various peptides and proteins, as described in Materials and Methods. No significant inhibitory effect was exerted by epidermal growth factor, methionine enkephalin, leucine enkephalin, vasopressin, vasoactive intestinal peptide (VIP), substance P, neurotensin, bombesin, cytochrome *c*, ubiquitin, aprotinin, leupeptin, pepstatin A, α_2-macroglobulin, somatostatin and α-melanocyte stimulating hormone (data not shown). However, some inhibition of binding was obtained with LIP1 (40 ± 5% inhibition; two independent determinations) and to a lesser extent with NGF (25 ± 3% inhibition; two independent determinations).

Cross-linking studies of ^{125}I-LIP2 bound to B5 cells showed the presence of a 145–150–kD species comigrating with the medium neurofilament protein subunit used as external marker and a 97-kD species comigrating with phospholipase B in SDS-polyacrylamide gels (Fig. 7). Given a molecular weight of about 4 kD for LIP2, this would suggest receptor forms of about 140–145 kD and 93 kD.

Induction of F-actin Redistribution by LIP1 and LIP2 in PC12 Cells

One of the earliest morphological events induced by NGF in PC12 cells is the redistribution of filamentous actin (F-actin) which occurs within minutes after the addition of the growth factor (Connolly et al., 1979; Paves et al., 1990). The formation of ruffles, accompanied by the redistribution of F-actin, may be one of the earliest steps in the process of neurite outgrowth in PC12 cells. We tested the possible effect of the peptides on the redistribution of F-actin. The two peptides induced striking morphological changes in PC12 cells within 2 min (Fig. 8) at all three peptide concentrations tested (10^{-7}, 10^{-8}, and 10^{-9} M). Fluorescent phalloidin specific for F-actin strongly labeled the stellate shapes generated in response to LIP1 and LIP2 at the cell periphery (Fig. 8 *C*, *D*). The distribution of F-actin into in-

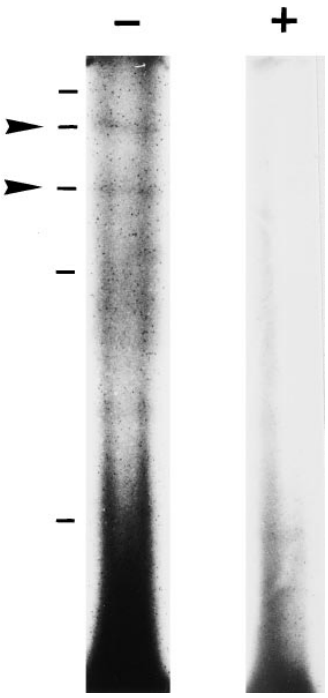

Figure 7. Characterization of LIP2 receptors by cross-linking. About 10^7 B5 cells were incubated for 2 h at 4°C with 100 nM ^{125}I-LIP2 in the absence (−) or presence (+) of excess unlabeled peptide. After washing and cross-linking with EDC, cells were subjected to electrophoresis as described in Materials and Methods. Arrows indicate cross-linked species. External markers are: neurofilament heavy subunit (200 kD), neurofilament medium subunit (145 kD), phospholipase B (97 kD), neurofilament light subunit (70 kD), and carbonic anhydrase (29 kD).

tensely fluorescent spikes in the cell periphery was similar but not identical to the more abundant ruffling induced by NGF (Fig. 8 *B*). Similar results were observed in PC12 cells that overexpress TrkA (data not shown). As a control, [Tyr^8] bradykinin was tested at 10^{-6} and 10^{-7} M and had no effect. Moreover, the effect of LIP1 and LIP2 is cell specific, since neither NGF nor the peptides induced F-actin rearrangement in B5 cells (Fig. 8 *F*). However, neither LIP1 nor LIP2 was able to induce neurite outgrowth either in PC12 cultures or in chick embryo DRG ganglia at 10^{-7}–10^{-9} M concentration, while dense neurite outgrowth was observable in NGF-treated PC12 cells and DRGs (data not shown).

Induction of Tyrosine Phosphorylation of the Trk Protein by LIP1 and LIP2 in PC12 and B5 Cells

The Trk protein, a 140-kD tyrosine kinase, was demonstrated to be the high affinity NGF receptor. NGF was shown first to trigger rapid phosphorylation and also to bind directly to Trk (Kaplan et al., 1991; Klein et al., 1991). Therefore, we looked for the possible induction of tyrosine phosphorylation of Trk by the two peptides. B5 cells and PC12 cells that overexpress TrkA were exposed to LIP1 or LIP2 for 2 min, and cell lysates were immunoprecipitated with an antibody generated against the COOH-terminal Trk peptide. Immunoprecipitates were subsequently probed with anti-phosphotyrosine (Ptyr) antibodies. Indeed, Trk was rapidly phosphorylated after addition of 10^{-9} M LIP1 or LIP2 in both PC12 and B5 cells, although peptide induction was less potent than NGF in PC12 cells. Fig. 9 shows a typical result which was reproduced in five independent experiments. There was no or little induction of Trk phosphorylation at 10^{-7} M peptide concentration in B5 cells (Fig. 9) nor in PC12 cells (data not shown).

Discussion

Putative Peptides from NGF and Neurotrophin Precursors

Peptide–hormone precursors are known to undergo post-translational cleavage to yield several biologically active peptides from one precursor molecule (Harris, 1989). It is generally accepted that the recognition sequence for endoproteolysis is a doublet of basic amino acids which bracket the peptide. The NGF precursor sequence contains four such sites (Fig. 1). Proteolysis at the proteolytic site (PS) 3 and PS4 liberates the NGF protein. Our working hypothesis was that processing may also occur at PS1 and PS2 in certain tissues, to yield two additional peptides of 29aa (LIP1) and 38aa (LIP2) from the short NGF precursor, which starts at the second initiator methionine codon and is the predominant precursor form in most tissues (Edwards et al., 1986). An NH_2-terminal 89aa peptide may also be generated from the long precursor, which starts at the first methionine codon and is the predominant form in the MSG. The neurotrophins (NT), brain derived neurotrophic factor (BDNF) (Leibrock et al., 1989), NT-3 (Maisonpierre et al., 1990), NT-4 (Hallböök et al., 1991), and NT-5 (Berkemeier et al., 1991; Ip et al., 1992) share 50–55% homology with NGF and are all synthesized from long precursor molecules. PS1 and PS2 are absent in pro-BDNF, and its corresponding −40 to −3 region shares only about 24% homology with LIP2. The NT-3 precursor lacks PS1, but PS2 and PS3 are conserved. Thus a LIP2-like peptide could be potentially generated from proNT-3, but it shares only about 31% homology with LIP2. The proNT-4 lacks both PS1 and PS2, and its corresponding −40 to −3 region shares about 26% homology with LIP2. The proNT-5 also lacks PS1 and PS2, and the corresponding −40 to −3 region shares about 21% homology with LIP2. Thus LIP1 and LIP2 may only be generated from the precursor sequence of proNGF.

LIP1 and LIP2 are Predominantly Expressed in the Intestine

The surprising finding was the detection of significant levels of LIP2 and, to a lesser extent, LIP1 in extracts of the intestine, whereas no LIP1 and low levels of LIP2 were detected in the MSG. Immunoprecipitation of LIP2 from an intestinal extract also indicates that the ELISA immunoreactive material is the free peptide. Furthermore, immunohistochemical evidence for the localization of LIP1 in intestinal endocrine cells that did not show any NGF immunoreactivity suggests a distinct role for this peptide in the intestine. The presence of LIP1 and LIP2 in the intestine was unexpected, because low levels of NGF protein were measured by the two site NGF ELISA in this tissue. More elevated NGF levels estimated at ~1 pg/mg protein were previously reported in the rat intestine (Westkamp and Otten, 1987). A low level of NGF synthesis has also been detected in vitro in intestinal epithelial cell lines (Varilek et al., 1995). The considerable levels of LIP1 and LIP2 in the intestine, as compared to their low levels in the MSG, suggests a differential expression of the two propeptides in these tissues.

No LIP1 or LIP2 was detected in whole brain extracts.

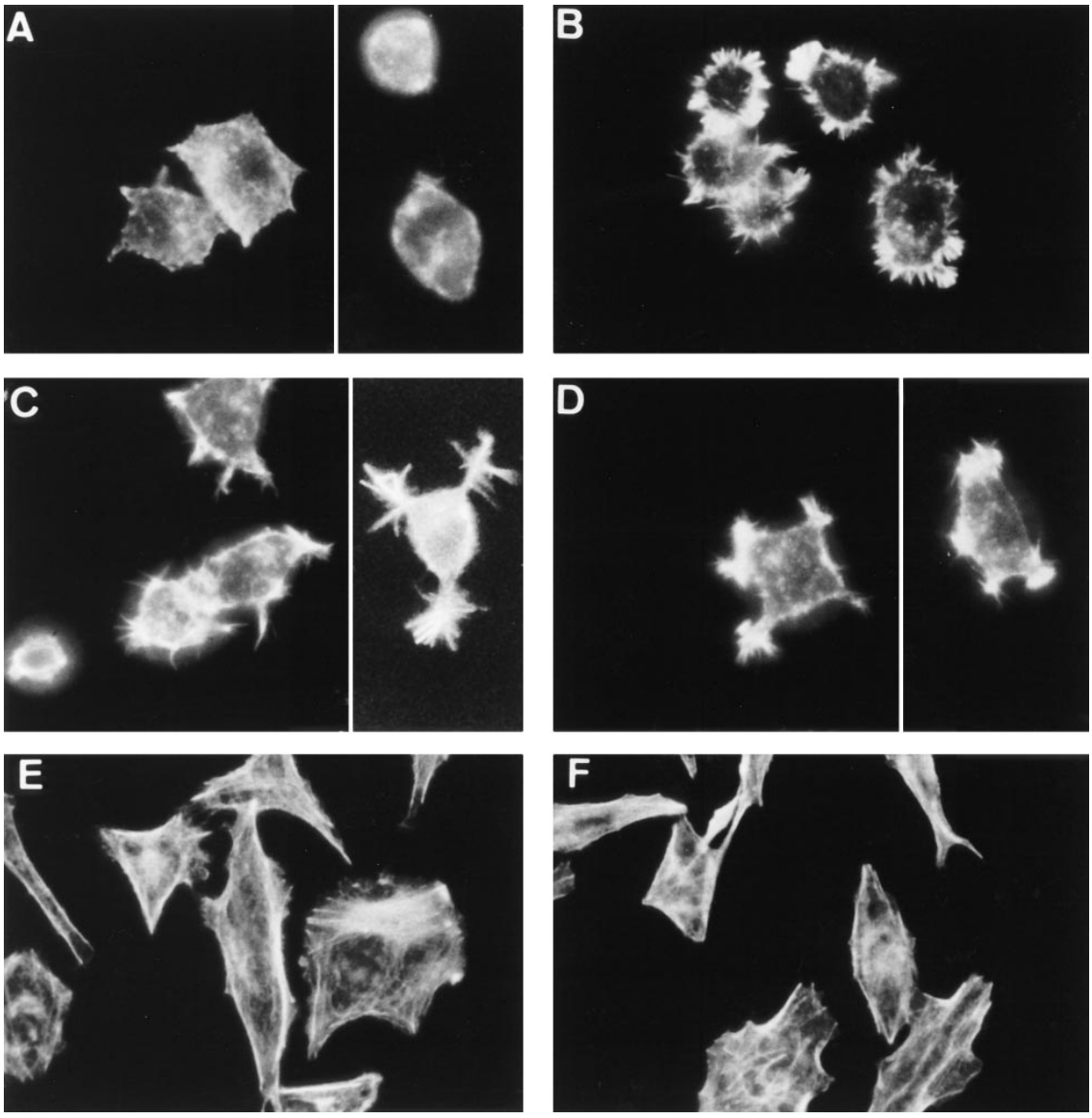

Figure 8. Effects of LIP1 and LIP2 treatment on F-actin distribution in PC12 cells and in human prostatic adenocarcinoma B5 cells. PC12 cells (*A–D*) and B5 cells (*E* and *F*) were incubated for 2 min in the absence (*A* and *E*) or presence of (*B*) 100 ng/ml NGF, (*C*) 10^{-8} M LIP1, and (*D* and *F*) 10^{-9} M LIP2. NGF and LIP1 also had no effect on B5 cells (results not shown).

In general, most neuropeptides are found peripherally and to a much lesser extent in brain extracts because of heterogeneity of the different regions of the brain (Lynch and Snyder, 1986). LIP2 was detectable in certain forebrain regions (cortex, hippocampus, and septum), however, other regions of the brain should be examined either by histochemistry or by immunoassay for the presence of these peptides. In a past study using purified antibodies against a shorter peptide (26aa) within the LIP1 sequence, immunoreactivity was detected in several regions of the brain, localizing within neurons in the cortex, hippocampus, and septum; this was interpreted as proNGF-like immunoreactivity (Senut et al., 1990). The question of the brain localization of these peptides should be reexamined using antibodies against the complete LIP1 peptide, as well as against LIP2. Taken together, these observations suggest that LIP1 and LIP2 may constitute peptides present in the gut–brain axis, as it was also observed for VIP, galanin, and somatostatin.

Evidence for Specific Receptors for LIP2

Specific binding of LIP2 was observed in several cell lines of human and rat origin. Scatchard analysis revealed two binding sites with different affinities for LIP2: a low affinity binding site with a K_d of $\sim 10^{-7}$–10^{-8} M and a high affinity binding site of $\sim 10^{-9}$ M. We can not exclude that other higher affinity components may exist, but they were undetected due to the low specific activity of the iodinated LIP2. The high affinity LIP2 receptor, with a K_d in the nanomolar range, resembles receptors described for other peptides in the digestive tract, such as VIP, galanin, and neurotensin (Laburthe et al., 1993). The physiological significance of the low affinity LIP2 receptor is intriguing. It

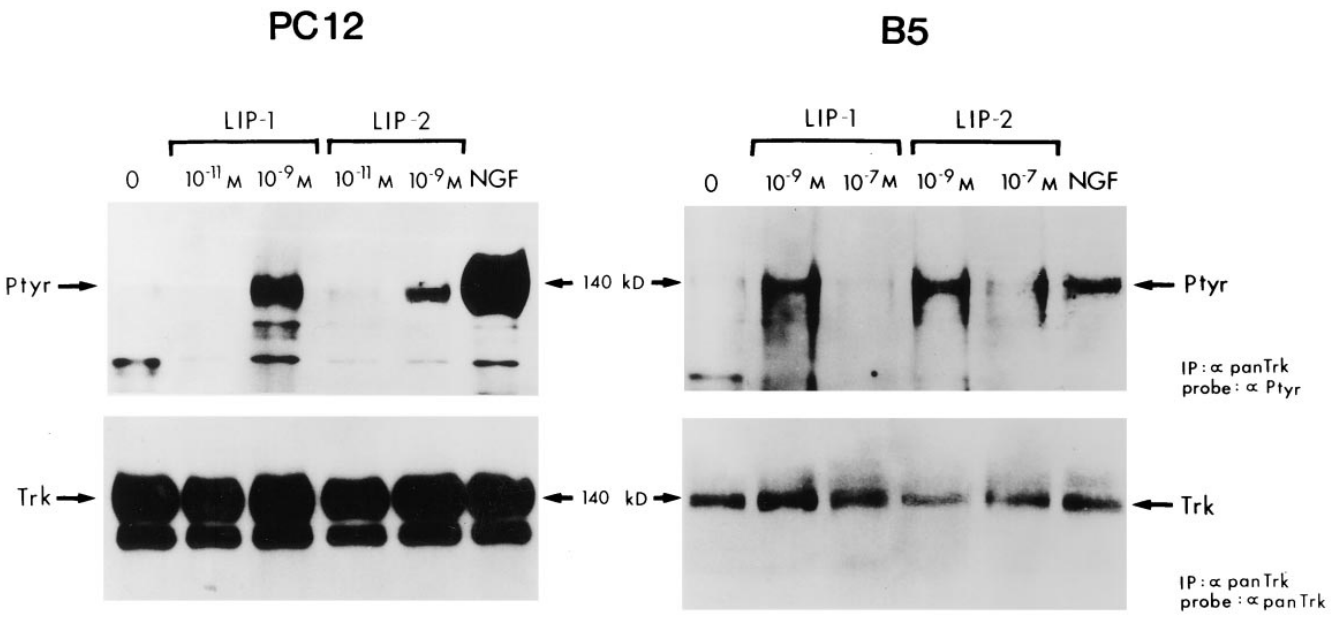

Figure 9. LIP1 and LIP2 stimulated tyrosine phosphorylation of the Trk protein. PC12 cells overexpressing TrkA and B5 cells were treated for 5 min with increasing concentrations of LIP1 and LIP2, or 200 ng/ml NGF, and lysed. Immunoprecipitation of the lysates with panTrk-21 antibody and immunoblot analysis using an antiphosphotyrosine antibody shows phosphorylation of Trk with 10^{-9} M LIP1 and LIP2 and 200 ng/ml NGF in both cell lines. The blots were stripped and reprobed with panTrk-203 antibody to show equal protein loading.

may be involved in mediating LIP2 endocytosis, since up to ~40% of the bound ^{125}I-LIP2 in acid-treated or azide-treated B5 and SH-SY5Y cells was internalized (Harvie, D., unpublished results). Low affinity binding was also observed for several gastrointestinal peptides whose receptors are coupled to G proteins (Laburthe et al., 1993).

In competition experiments, there was no significant inhibition of the binding of LIP2 by any of the peptides or proteins that we tested, other than a significant inhibitory effect by LIP1. This may suggest that LIP1 and LIP2 compete for the same receptor subtype. Competition experiments in the presence of 2 μM NGF and 10 nM ^{125}I-LIP2 did not show any significant inhibition of ^{125}I-LIP2 binding, which suggests that LIP2 does not bind at the same sites as NGF. No transcripts coding for the low affinity NGF receptor were detected in B5 (MacGrogan et al., 1992). However, B5 cells express TrkA, as confirmed by Western blot with a TrkA specific antibody (anti-TrkAin; Pflug, B. and D. Djakiew, unpublished results), and they may also express TrkB or TrkC. In view of the present results demonstrating that LIP1 and LIP2 induce tyrosine phosphorylation of Trk, the possibility that these peptides may bind directly to Trk, as does NGF, merits further examination. Our binding studies, as well as the identification of specific molecular weight species in cross-linking experiments, strongly suggest the presence of specific receptors for LIP2 in several cell lines and would therefore argue in favor of a physiological role for this peptide.

Physiological Action of LIP1 and LIP2

In vitro, unlike NGF, LIP1 and LIP2 did not elicit neurite outgrowth either in PC12 cells or in DRG explants. In vivo, it is well established that intracerebroventricular injections of NGF or NGF antibodies into neonatal rats causes significant changes in cholinergic enzyme activities in the septum, cortex, hippocampus, and striatum. Intracerebroventricular injections of LIP1 into neonatal hypothyroid rats increased choline acetyltransferase (ChAT) and acetylcholinesterase by 24–40% in the cortex, septum, and hippocampus. Intraventricular injections of LIP2 increased ChAT by 15% only in the cortex and not in the hippocampus or septum. However, unlike NGF, neither LIP1 nor LIP2 had any effect on the ChAT activity of fetal rat septal neuronal cultures (Clos and Dicou, 1997).

Since neurite formation and ChAT induction are late events in the cellular response to exogenous signals, we next investigated the possible effects of LIP1 and LIP2 on early cellular events. One such event is F-actin redistribution. Upon LIP1 and LIP2 treatment, PC12 cells respond by a rapid sequence of changes in cell surface architecture, leading to a redistribution of F-actin, as previously shown for NGF (Connolly et al., 1979; Paves et al., 1990). No F-actin redistribution was observed either by the peptides or by NGF in B5 cells. The differences in the effects between the two cell lines may reflect differences between a neuronal cell line (PC12) and an epithelial-like cell line (B5).

Another early cellular event is tyrosine phosphorylation of the *trk* proto-oncogene product within 1 min of exposure to NGF (Kaplan et al., 1991). LIP1 and LIP2 can also induce Trk phosphorylation in B5 cells as well as in PC12 cells that overexpress TrkA. Thus activation of the Trk tyrosine kinase receptor seems to be a possible mechanism of signal transduction for LIP1 and LIP2. Interestingly, Trk phosphorylation by LIP1 and LIP2 was more pronounced at 1 nM than at 100 nM in B5 cells, as well as in PC12 overexpressing TrkA. This may be due to down regulation of phosphorylation at above optimal peptide con-

centrations. A similar effect has been observed for NT-3 interaction with TrkC (Tsoulfas et al., 1993) and for other nonneurotrophin related ligand–receptor interactions (Zolfaghari and Djakiew, 1996). A bell-shaped hormone response curve resulting in inhibition of the transducing signal at high ligand concentrations was also observed for the human growth hormone receptor (Fuh et al., 1992).

In summary, we provide evidence for the presence of two propeptides derived from the NGF precursor, LIP1 and LIP2, in the intestine and the localization of LIP1 in endocrine cells. We also demonstrate that they are biologically active, since they can induce two early events in the cellular response: (*a*) F-actin rearrangement and (*b*)Trk phosphorylation. Investigation for possible induction of other intracellular signalling systems by these peptides may reveal preferential mechanisms of activation.

We thank the two anonymous reviewers for their constructive comments and Dr Y. Jacques (INSERM U211, Nantes, France) for invaluable aid with the Graphit program.

This work was supported by grants from the Association pour la Recherche sur les Tumeurs Prostatiques and the Association pour la Recherche sur le Cancer to E. Dicou.

Received for publication 8 March 1996 and in revised form 23 August 1996.

References

Berkemeier, L.R., J.W. Winslow, D.R. Kaplan, K. Nikolics, D.V. Goeddel, and A. Rosenthal. 1991. Neurotrophin-5: a novel neurotrophic factor that activates trk and trkB. *Neuron.* 7:857–866.

Bookstein, R., J.-Y. Shew, P.-L. Chen, P. Scully, and W.-H. Lee. 1990. Suppression of tumorigenicity of human prostate carcinoma cells by replacing a mutated RB gene. *Science (Wash. DC).* 247:712–715.

Clos, J., and E. Dicou. 1997. Two peptides derived from the nerve growth factor precursor enhance cholinergic enzyme activities in vivo. *Dev. Brain Res.* In Press.

Connolly, J.L., L.A. Greene, R.R. Viscarello, and W.D. Riley. 1979. Rapid, sequential changes in surface morphology of PC12 pheochromocytoma cells in response to nerve growth factor. *J. Cell Biol.* 82:820–827.

Dicou, E. 1989. Interaction of antibodies to synthetic peptides of proNGF with in vitro-synthesized NGF precursors. *FEBS Lett.* 255:215–218.

Dicou, E., J. Lee, and P. Brachet. 1986. Synthesis of nerve growth factor mRNA and precursor protein in the thyroid and parathyroid glands of the rat. *Proc. Natl. Acad. Sci. USA.* 83:7084–7088.

Dicou, E., J. Lee, and P. Brachet. 1988. Co-localization of the nerve growth factor precursor protein and mRNA in the mouse submandibular gland. *Neurosci. Lett.* 85:19–23.

Dicou, E., R. Houlgatte, J. Lee, and B. von Wilcken-Bergmann. 1989. Synthesis of chimeric mouse nerve growth factor precursor and human β-nerve growth factor in *E. coli*: Immunological properties. *J. Neurosci. Res.* 22:13–19.

Dicou, E. 1992. Nerve growth factor precursors in the rat thyroid and hippocampus. *Mol. Brain Res.* 14:136–138.

Dicou, E., D. Hurez, and V. Nerrière. 1993. Natural autoantibodies against the nerve growth factor in autoimmune diseases. *J. Neuroimmunol.* 47:159–168.

Edwards, R.H., M.J. Selby, and W.J. Rutter. 1986. Differential RNA splicing predicts two distinct nerve growth factor precursors. *Nature (Lond.).* 319: 784–787.

Fuh, G., B.C. Cunningham, R. Fukunaga, S. Nagata, D.V. Goeddel, and J.A. Wells. 1992. Rational design of potent antagonists to the human growth hormone receptor. *Science (Wash. DC).* 256:1677–1680.

Hallböök, F., C.F. Ibanez, and H. Persson. 1991. Evolutionary studies of the nerve growth factor family reveal a novel member abundantly expressed in *Xenopus* ovary. 1991. *Neuron.* 6:845–858.

Harris, R.B. 1989. Processing of pro-hormone precursor proteins. *Arch. Biochem. Biophys.* 275:315–333.

Hempstead, B.L., S.J. Rabin, L. Kaplan, S. Reid, L.F. Parada, and D.R. Kaplan. 1992. Overexpression of the *trk* tyrosine kinase rapidly accelerates nerve growth factor-induced differentiation. *Neuron.* 9:883–896.

Ip, N.Y., C.F. Ibanez, S.H. Nye, J. McClain, P.F. Jones, D.R. Gies, L. Belluscio, M.M. Le Beau, R. Espinosa III, S.P. Squinto, et al. 1992. Mammalian neurotrophin-4: structure, chromosomal localization, tissue distribution, and receptor specificity. *Proc. Natl. Acad. Sci. USA.* 89:3060–3064.

Kaplan, D.R., D. Martin-Zanca, and L.F. Parada. 1991. Tyrosine phosphorylation and tyrosine kinase activity of the *trk* proto-oncogene product induced by NGF. *Nature (Lond.).* 350:158–160.

Klein, R., S. Jing , V. Nanduri, E. O'Rourke, and M. Barbacid. 1991. The *trk* proto-oncogene encodes a receptor for nerve growth factor. *Cell.* 65:189–197.

Laburthe, M., P. Kitabgi, A. Couvineau, and B. Amiranoff. 1993. Peptide receptors and signal transduction in the digestive tract. *In* Handbook of Experimental Pharmacology. Vol. 106. Gastrointestinal Regulatory Peptides. D.R. Brown, editor. Springer-Verlag, Berlin. 133–176.

Laemmli, U.K. 1970. Cleavage of structural proteins during the assembly of the head of bacteriophage T4. *Nature (Lond.).* 227:680–685.

Leibrock, J., A.H. Lottspeich, M. Hofer, B. Hengerer, P. Masiakowski, H. Thoenen, and Y.-A. Barde. 1989. Molecular cloning and expression of brain-derived neurotrophic factor. *Nature (Lond.).* 341:149–152.

Lynch D.R., and S.H. Snyder. 1986. Neuropeptides: multiple molecular forms, metabolic pathways and receptors. *Annu. Rev. Biochem.* 55:773–799.

Maisonpierre, P.C., L. Belluscio, S. Squinto, N.Y. Ip, M.E. Furth, R.M. Lindsay, and G.D. Yancopoulos. 1990. Neurotrophin-3: a neurotrophic factor related to nerve growth factor and brain-derived neurotrophic factor. *Science (Wash. DC).* 247:1446–1451.

McGrogan, D., J.-P. Saint-André, and E. Dicou. 1992. Expression of nerve growth factor and nerve growth factor receptor genes in human tissues and in prostatic adenocarcinoma cell lines. *J. Neurochem.* 59:1381–1391.

Meakin, S.O., and E.M. Shooter. 1992. The nerve growth factor family of receptors. *Trends Neurosci.* 15:323–331.

Paves, H., T. Neuman, M. Metsis, and M. Saarma. 1990. Nerve growth factor induces rapid redistribution of F-actin in PC12 cells. *FEBS Lett.* 235:141–143.

Pflug, B., C. Dionne, D.R. Kaplan, J. Lynch, and D. Djakiew. 1995. Expression of a Trk high affinity nerve growth factor receptor in the human prostate. *Endocrinology.* 136:262–268.

Scott, J., M. Selby, M. Urdea, M. Quiroga, G.I. Bell, and W.J. Rutter. 1983. Isolation and nucleotide sequence of a cDNA encoding the precursor of mouse nerve growth factor. *Nature (Lond.).* 302:538–540.

Senut, M-C., Y. Lamour, J. Lee, P. Brachet, and E. Dicou. 1990. Neuronal localization of the nerve growth factor precursor-like immunoreactivity in the rat brain. *Int. J. Dev. Neurosci.* 8:65–80.

Suter, U., J.V. Heymach, and E.M. Shooter. 1991. Two conserved domains in the NGF propeptide are necessary and sufficient for the biosynthesis of correctly processed and biologically active NGF. *EMBO (Eur. Mol. Biol. Organ.) J.* 10:2395–2400.

Thoenen, H. 1991. The changing scene of neurotrophic factors. *Trends Neurosci.* 14:165–170.

Tsoulfas, P., D. Soppet, E. Escandon, L. Tessarollo, J.-L. Mendoza-Ramirez, A. Rosenthal, K. Nikolics, and L.F. Parada. 1993. The rat trkC locus encodes multiple neurogenic receptors that exhibit differential response to neurotrophin-3 in PC12 cells. 1993. *Neuron.* 10:975–990.

Ullrich, A., A. Gray, C. Berman, and T.J. Dull. 1983. Human β-nerve growth factor gene sequence highly homologous to that of mouse. *Nature (Lond.).* 303:821–825.

Varilek, G.W., G.A. Neil, W.P. Bishop, J. Lin, and N.J. Pantazis. 1995. Nerve growth factor synthesis by intestinal epithelial cells. *Am. J. Physiol.* 269: G445–G452.

Weskamp, G., and U. Otten. 1987. An enzyme-linked immunoassay for nerve growth factor (NGF): a tool for studying regulatory mechanisms involved in NGF production in brain and in peripheral tissues. *J. Neurochem.* 48:1779–1786.

Wulf, E., A. Dobeban, F.A. Bautz, H. Faulstich, and T.H. Wieland. 1979. Fluorescent phallotoxin. A tool for the visualization of cellular actin. *Proc. Natl. Acad. Sci. USA.* 76:4498–4502.

Zolfaghari, A., and D. Djakiew. 1996. Inhibition of chemomigration of a human prostatic carcinoma cell line (TSU-pr1) by inhibition of epidermal growth factor receptor function. *Prostate.* 28:232–238.